Design and Control of Pneumatic Systems for Soft Robotics: A Simulation Approach

Matheus S. Xavier, Andrew J. Fleming, and Yuen K. Yong

***Abstract*—Pressure control plays a major role in the overall performance of fluid-driven soft robots. Due to the increasing demand for higher speed actuation and precision, a need exists for a practical design methodology that converts actuator performance specifications to a set of minimum pneumatic specifications, such as receiver volume and pressure, and valve conductance. This article presents a systematic parameter selection approach for pneumatic soft robotic systems by taking into consideration the desired closed-loop pressure responses. The two controllers under evaluation here are the PI controller with anti-windup and the on-off controller with hysteresis. Simulations are developed within Simscape Fluids to evaluate the effect of physical components and controller parameters on the actuator performance. The proposed parameter selection procedures are then applied on three soft actuators and their closed-loop pressure responses are experimentally evaluated. The measured pressure responses are in close agreement with the simulations and satisfy the rise time specifications.**

***Index Terms*—Modeling, control, and learning for soft robots, soft sensors and actuators, hydraulic/pneumatic actuators.**

I. Introduction

SOFT robots are made of highly deformable and compliant materials. They show high dexterity and safety, are physically resilient and can adapt to delicate objects and environments due to their conformal deformation [1], [2]. Many soft robots are fabricated from soft fluidic actuators, where actuation is performed using pneumatics or hydraulics [3], [4]. The strong nonlinearities in soft actuators and their complex geometries are the key challenges in developing accurate mathematical models [5], [6].

The nonlinearities arising from the hyperelasticity of soft materials are compounded by the nonlinearities from the pneumatic actuation, which includes the compressibility of air, the nonlinear relationship between pressure and flow of the valves and a non-trivial time delay [7], [8]. Regardless of the soft actuator, the pneumatic system critically affects the pressure dynamics of soft actuators [9], [10]. Therefore, pressure control plays a major role in the overall performance of soft robots [11], [12].

Manuscript received February 10, 2021; accepted May 24, 2021. Date of publication June 4, 2021; date of current version June 15, 2021. This letter was recommended for publication by Associate Editor H. Rodrigue and Editor C. Laschi upon evaluation of the reviewers' comments. *(Corresponding author: Matheus S. Xavier.)*

The authors are with the Precision Mechatronics Laboratory at the School of Electrical Engineering and Computer Science, The University of Newcastle, Callaghan, NSW 2308, Australia (e-mail: Matheus.Xavier@uon.edu.au; andrew.fleming@newcastle.edu.au; yuenkuan.yong@newcastle.edu.au).

Digital Object Identifier 10.1109/LRA.2021.3086425

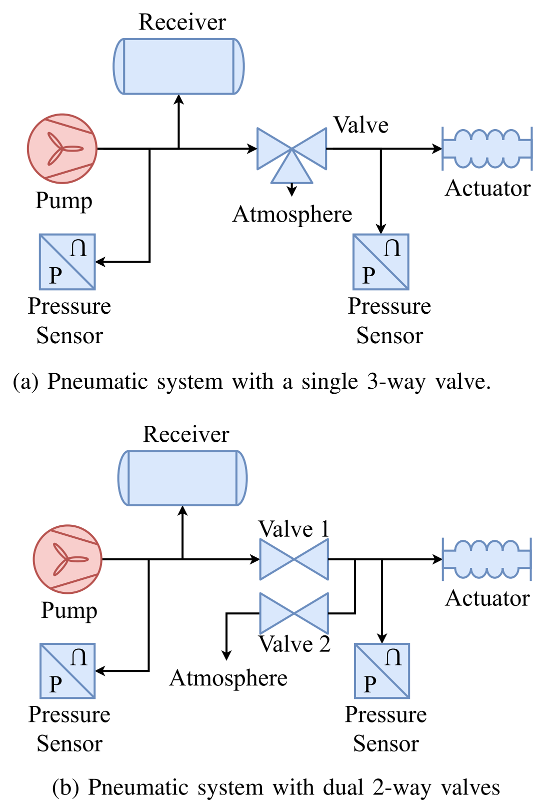

Fig. 1. Pneumatic systems with the two common valve configurations in the soft robotics literature. (a) Pneumatic system with a single 3-way valve. (b) Pneumatic system with dual 2-way valves.

The main components of a pneumatic system are the source for generating pressurized air, the pneumatic lines for connection, and the valves for controlling flow direction [9], [13]. Pressure control in the soft actuator is usually achieved with 3/2 (3-way, 2-position) or 2/2 (2-way, 2-position) solenoid valves [11], [14], [15], as shown in Fig. 1. The addition of an air receiver improves response speed and efficiency while minimizing the required pump flow rate [9], [10]. The most popular pneumatic control architecture for soft robotics is the fluidic control board, which consists mainly of a diaphragm pump and a set of 3/2 solenoid valves. Pulse-Width Modulation (PWM) is used to control the pressure of fluid passing through the valves, while pressure sensors are used for feedback control.

Most practical fluid-powered soft robots use experimentally-tuned strategies to control the motion of soft actuators. This approach has been explored in soft snake-like [16], worm-like

[17], soft-bodied fish [18] and manta ray [19] robots. PID controllers have been considered in [15], [20]–[22]. In [20], the PID controller was shown to be more suitable than a sliding mode controller for trajectory tracking in an experimental setup, at the expense of higher overshoot and lower robustness to external forces. Conversely, the sliding mode controller with a PID sliding surface in [23] reduces vibrations on deactuation in comparison to a model-free PID controller. In [24], automatic tuning of ordinary, piecewise and fuzzy PID controllers using a heuristic-based coordinate descent algorithm is proposed. In [16], on-off control is used to intermittently turn the pump on and off and keep the pressure relatively constant during robot locomotion. In [17], [25], this control is used to actuate the valves in order to generate peristaltic locomotion.

A number of advanced control techniques have been proposed for soft robotic actuators, such as sliding modes [7], [20], [26], model reference adaptive [11] and robust backstepping [8], [15]. However, these are only effective if the response time is not limited by the dynamics of the pneumatic system. To ensure that the open-loop response time is sufficient for a given application, a significant need exists for a methodology that chooses a set of minimum pneumatic specifications, such as the pump, receiver, and valve characteristics. A step towards resolving this issue is the work of [9] in which the authors introduce a mathematical model of the pneumatic system for the selection of source, valve and pneumatic lines.

The contributions of this article include a practical process for pneumatic component and controller design, a set of generalized design curves for initialization, and a comparison of valve configurations and pressure control schemes. Simscape Fluids is employed to evaluate the effect of pneumatic components in the pressure response of soft actuators. The valves under consideration include readily available solenoid valves in three-way or two-way configurations. Once the parameters of the pneumatic system are selected, control strategies using experimentally-tuned on-off and PI controllers are compared for pressure regulation of soft actuators. The results show that by considering the pneumatic limitations, appropriate parameter values can be selected to satisfy requirements on the actuator response.

II. Pneumatic Control Strategies

A. PI Controller With Anti-Windup

Pressure control in the actuator is performed by controlling the duty cycle of the valve. For a PID controller, the duty cycle u of the valve is [27]

$$u = K_p e(t) + K_i \int_{t_0}^{t} e(\tau) d\tau + K_d \frac{\mathrm{d}e(t)}{\mathrm{d}t} \quad (1)$$

where $e(t) = P_{ref}(t) - P(t)$ is the difference between the reference pressure $P_{ref}(t)$ and the real-time pressure $P(t)$, and K_p, K_i and K_d are the proportional, integral and derivative gains of the PID controller.

Initially, derivative and integral gains are set to zero. Inspired by the Ziegler-Nichols oscillation method, the proportional gain is increased until the control system reaches an oscillatory behavior. Next, the integral gain is increased to reduce tracking error. The proportional and integral gains are then tuned to improve tracking performance. In the pressure control of soft fluidic actuators, high frequency control errors are present due to PWM switching, measurement noise and set-point changes. Consequently, the derivative mode yields large control signals and is not included in the controller design.

Actuator saturation plays a major role in pneumatic control as the duty cycle is limited between zero and one and large set-point changes are usually of interest. Without anti-windup, the state of the integrator can reach an unacceptable high value leading to poor transient response [27]. Here, anti-windup is implemented using conditional integration (integrator clamping) [28].

B. On-Off Controller With Hysteresis

For on-off control (bang-bang control), the valve is on $(u = 1)$ to increase the pressure at maximum rate until the reference pressure is exceeded, at which point the valve is turned off $(u = 0)$ until the pressure falls below the threshold. In order to prevent frequent operation of the on–off mechanism, hysteresis introduces a dead-band around the set-point where there is no control action. For the 3-way valve system, two states are considered:

$$\text{State ON}: \; P(t) < P_{ref}(t) - h \Rightarrow e(t) > h \quad (2)$$

$$\text{State OFF}: \; P(t) > P_{ref}(t) + h \Rightarrow e(t) < -h \quad (3)$$

where h is half the size of the hysteresis band.

C. Moving Average Filter

The 3/2 valve system implies constantly inflating and deflating each actuator, which causes the pressure in the actuator to continuously oscillate around its target. Therefore, a moving average filter for the last 10 pressure measurements is included in the LabVIEW subroutines to smooth the effects of the pulse-width modulation and minimize switching events due to sensor noise.

III. Parameter Analysis for Pneumatic Systems

Simulations have been developed with the package Simscape Fluids within MATLAB/Simulink. An example of a pneumatic soft actuator system is provided in the Appendix. The actuators are modeled as constant volume chambers, which is reasonable for actuators with low levels of ballooning, including fiber-reinforced actuators, fast pneumatic network actuators, 3D/4D-printed bending and helical actuators, and actuators fabricated with harder silicone rubbers [5], [8]. The characteristics of the air pump, receiver and valves are analyzed and discussed below.

A. Air Pump

The open-loop pressure dynamics for constant flow sources directly charging the actuator are shown in Figs. 2(a) and 2(b) for two actuator volumes spanning typical ranges in soft robotics. While these results can be used in initial designs or flow-controlled pneumatic systems, commercial air pumps show reduced flow with increased pressures. The characteristics of

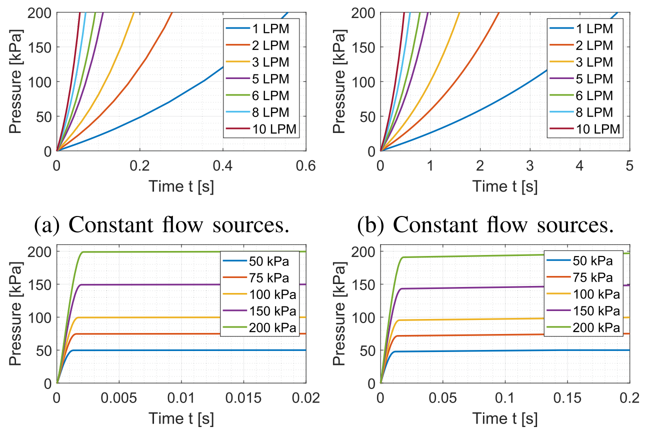

(a) Constant flow sources. (b) Constant flow sources.

(c) Constant receiver pressures. (d) Constant receiver pressures.

Fig. 2. Open-loop pressure step responses of soft actuators with volumes V_A of 10 mL (left column) and 100 mL (right column). The top row plots pressure responses with constant flow sources between 1 LPM (liters per minute) and 10 LPM. The bottom row plots pressure responses with receiver pressures between 50 kPa and 200 kPa.

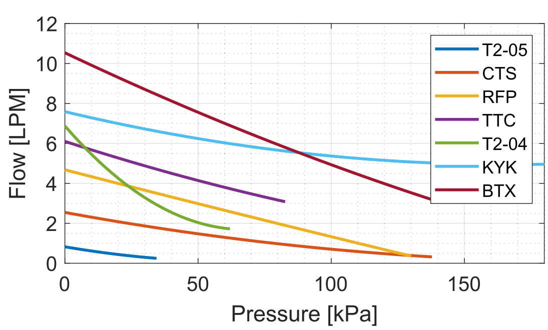

Fig. 3. Commercial air pump characteristics: T2-05 (0.8 LPM), CTS (2.5 LPM), RFP32H05R (4.8 LPM), TTC (6 LPM), T2-04 (7.5 LPM), KYK50BPM (10 LPM) and BTX Connect (11 LPM).

a variety of commercial air pumps have been collected from datasheets or determined using flow (AWM5000) and pressure (SEN0257, DFRobot) sensors, as depicted in Fig. 3. In addition to the decreasing flow with pressure, air pumps are usually accompanied by pressure regulators or relief valves to avoid pressure build-up in the lines, which increases cost and reduces energy efficiency.

B. Receiver (Reservoir or Gas Tank)

To mitigate the aforementioned issues with a pump, a receiver is added to the system. The receiver improves response time, efficiency, and minimizes the required pump flow rate [10], [29]. As shown in Figs. 2(c) and 2(d), the presence of the receiver provides fast actuation with rise times below 20 ms.

C. Valves

For pneumatic systems with a receiver, the valve largely dictates the actuator pressure response. According to ISO standard 6358 [9], [30], the flow rate through a valve is given by

$$Q = uC\Psi P_{high} \tag{4}$$

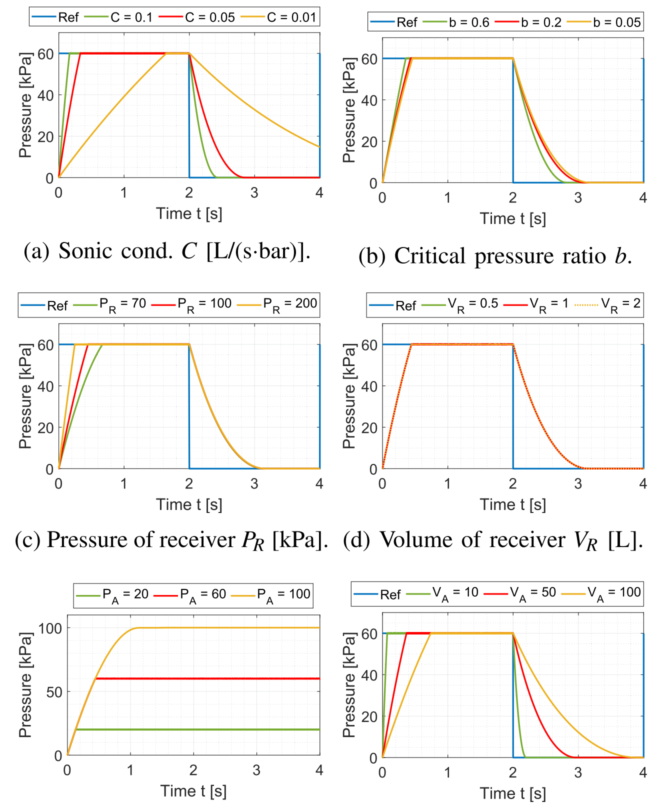

(a) Sonic cond. C [L/(s·bar)]. (b) Critical pressure ratio b.

(c) Pressure of receiver P_R [kPa]. (d) Volume of receiver V_R [L].

(e) Pressure of actuator P_A [kPa]. (f) Volume of actuator V_A [mL].

Fig. 4. Effect of valve, receiver and actuator characteristics on the pressure dynamics. Simulation results are obtained using an on-off controller with $h = 0.1$ kPa. The reference pressure response is simulated with a 60 mL actuator, a 2 L receiver at 100 kPa, and a valve with sonic conductance of 0.04 L/(s · bar) and critical pressure ratio of 0.1.

$$\Psi = \begin{cases} \sqrt{1 - \left(\dfrac{\frac{P_{low}}{P_{high}} - b}{1-b}\right)^2} & , \ \dfrac{P_{low}}{P_{high}} \geq b \\ 1 & , \ \dfrac{P_{low}}{P_{high}} < b \end{cases} \tag{5}$$

where u is the duty cycle, P_{high} and P_{low} are the absolute upstream and downstream pressures, C is the sonic conductance and b is the critical pressure ratio. During charging, $P_{high} = P_R$ and $P_{low} = P_A$, where P_R is the receiver pressure and P_A is the actuator pressure. During discharging, $P_{high} = P_A$ and $P_{low} = P_{atm}$, where P_{atm} is the atmospheric pressure.

D. General Guidelines

In this section, an on-off controller with $h = 0.1$ kPa is used to evaluate the system parameters. The on-off controller can transfer the system from an initial state to a target state in minimum time (time-optimal control law) since the control variable is either at its upper or lower bound [31].

As shown in Fig. 4(a), the sonic conductance has a large influence in the rise time of the response. Larger values of C lead to faster response, while the critical pressure ratio has a smaller impact on the transient characteristics (Fig. 4(b)). As shown in Fig. 4(d), the receiver volume has little impact on the response as long as it is above 10 times the volume of the actuator. As

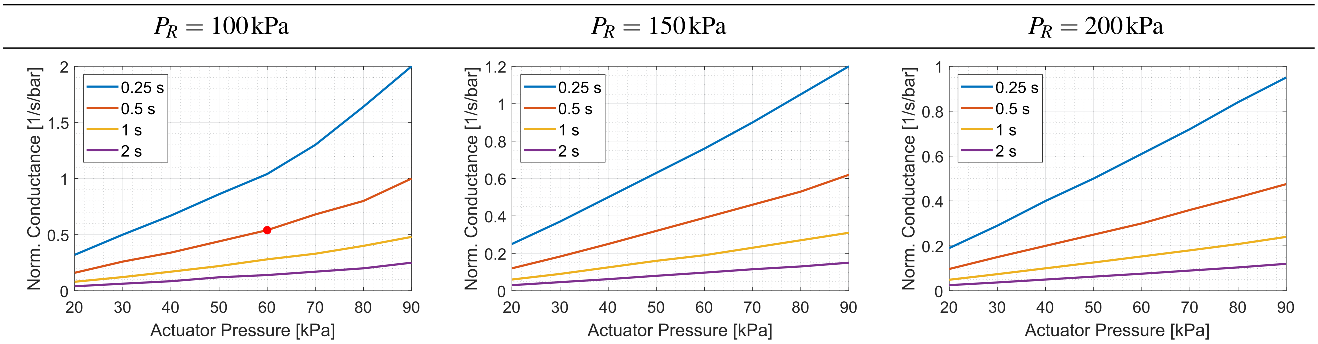

Fig. 5. Normalized sonic conductance $\bar{C} = C/V_A$ for system with receiver at three different pressures. The actuator pressure is varied between 20 kPa and 90 kPa in steps of 10 kPa and conductance values are interpolated for four desired rise times.

Algorithm: Parameter Selection

Step 1: Define actuator characteristics and requirements:
- Maximum pressure P_A and volume V_A of the actuator.
- Desired rise time T_{rise} of the actuator response $T_{rise} \in \{0.25, 0.5, 1, 2\}$s.
- Maximum number of actuation cycles per minute N.

Step 2: Select receiver parameters:
- $V_R > 10 \times V_A$ (see note 1 below).
- $P_R > 1.2 \times P_A$ (note 2) and $P_R \in \{100, 150, 200\}$kPa.

Step 3: Select valve sonic conductance:
- Use Fig. 5 to determine the normalized conductance $\bar{C}$ for desired P_A and T_{rise}.
- For the corresponding $\bar{C}$, select $C \geq \bar{C} \times V_A$.

Step 4: Select valve configuration:
- 2-way for higher accuracy and energy efficiency.
- 3-way for a low-cost and simple implementation.

Step 5: Select air pump parameters (Fig. 3):
- 2-way: $Q_{Pump}(P_R) \geq Q_{req}$ from (8).
- 3-way: $Q_{Pump}(P_R) \geq Q_{req,3way}$ from (9).

expected from equations (4) and (5), higher receiver pressure leads to higher flow into the soft actuator and, therefore, a faster response (Fig. 4(c)). In contrast, a slower response is obtained by increasing the actuator pressure or volume (Figs. 4(e)–(f)).

Note 1: 1 L, 1.5 L or 2 L recommended due to large availability.

Note 2: This condition ensures the receiver pressure does not drop below the actuator pressure and the slew rate of the actuator response does not significantly differ from its maximum value.

IV. Parameter Selection for Pneumatic Systems

The volume of the receiver and the critical pressure ratio of the valve do not significantly affect the pressure response of the system. These parameters are therefore excluded from the selection procedure below. The algorithm above summarizes the design for the main components of pneumatic systems.

A. Selection of Valve Configuration

For the system with dual 2-way valves, the first valve is used for charging the actuator while the second valve is used for discharging. Compared to systems with a single 3-way valve,

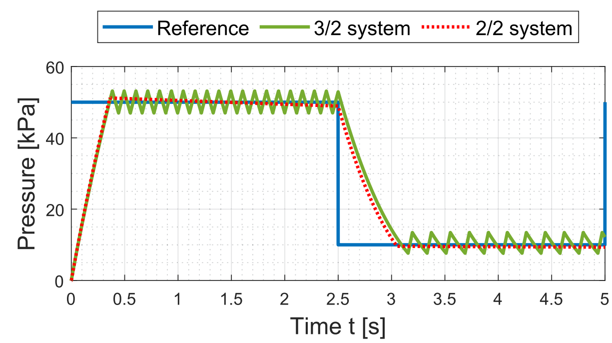

Fig. 6. Comparison of pressure responses for systems with a single 3/2 valve and dual 2/2 valves. An on-off controller with $h = 2$ is used. The sonic conductance of the valves is 0.04 L/(s · bar) and the critical pressure ratio is 0.1.

TABLE I
Comparison of Pneumatic System Setups

Setup	Cost (AUD)	Lifetime	Accuracy	Control
3/2 on-off valve	∼$40-70	Low	Medium	Simple
2/2 on-off valves	∼$80-150	Medium	High	Complex
2/2 prop. valves	∼$300-500	High	High	Complex

these systems allow for an additional state where both valves are off and there is no flow from the receiver or to atmosphere. The comparison between a single 3/2 (3-way, 2-position) valve system and dual 2/2 (2-way, 2-position) valve system in Fig. 6 shows that the dual 2/2 system achieves identical transient performance, i.e. identical rise and fall time. This also applies to 4/2, 5/2, 4/3 and 5/3 valves with the same sonic conductance and critical pressure ratio values.

Table I provides a comparison of pneumatic systems with these two valve configurations. Although offering lower cost and easier implementation, 3-way valve systems constantly inflate and deflate the soft actuator during pressure regulation, consequently 2-way valve systems allow for more energy-efficient pneumatic controllers and improved lifetime of the valves.

B. Selection of Air Pump

From mass conservation, the net flow into the actuator Q_A is [10], [32]

$$Q_A = \frac{V_A}{\gamma P_A} \frac{\mathrm{d}P_A}{\mathrm{d}t} \tag{6}$$

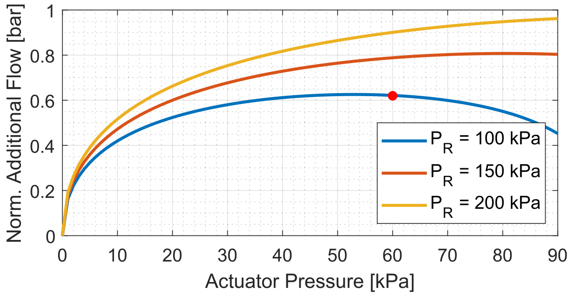

Fig. 7. Normalized additional flow $\overline{Q}_{add} = Q_{add}/C$ required for pressure regulation with 3-way valve systems.

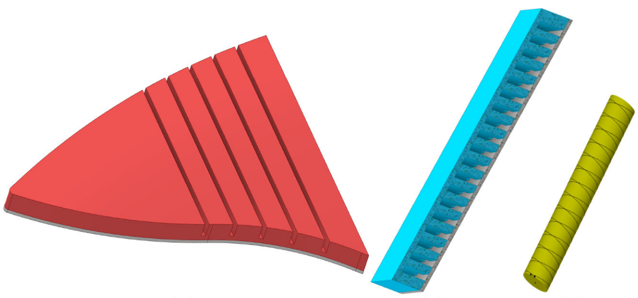

Fig. 8. Soft pneumatic actuators: (a) cownose ray-inspired fin with fast pneumatic network (PneuNet) design ($V_A = 60$ mL), (b) cross-section view of a slow PneuNet actuator ($V_A = 30$ mL) and (c) three-chambered omnidirectional actuator with double wrapping of fiber ($V_A = 5$ mL).

where γ is the polytropic index, here $\gamma = 1.4$ (isentropic process) as this value shows excellent agreement to Fig. 2(a). Since $Q_A = dV_{air}/dt$, where V_{air} is the volume of air consumed during one actuation cycle from atmospheric pressure P_{atm} to the desired pressure P_A, (6) yields

$$V_{air} = \frac{V_A}{\gamma} \ln\left(\frac{P_A}{P_{atm}}\right) \quad (7)$$

For N actuation cycles per minute, the required flow Q_{req} [LPM] from the air pump to keep the receiver at constant pressure is

$$Q_{req} = \frac{N \times V_A}{\gamma} \ln\left(\frac{P_A}{P_{atm}}\right) \quad (8)$$

For 3-way valves, an additional volume of air is consumed during regulation due to frequent switching and release of air to atmosphere. The duty cycle for pressure regulation can be calculated using (4)–(6) by setting dP_A/dt equal to zero. The resulting additional flow normalized to sonic conductance $\overline{Q}_{add} = Q_{add}/C$ is shown in Fig. 7. Therefore, the total required flow for 3-way valves $Q_{req,3way}$ is

$$Q_{req,3way} = Q_{req} + Q_{add} \quad (9)$$

where $Q_{add} = 60 \times \overline{Q}_{add} \times C$ in LPM.

V. Experimental Implementation

In this section, an example of the parameter selection procedure is provided. The PI and on-off control strategies in Sec. II are implemented on three types of soft pneumatic actuators

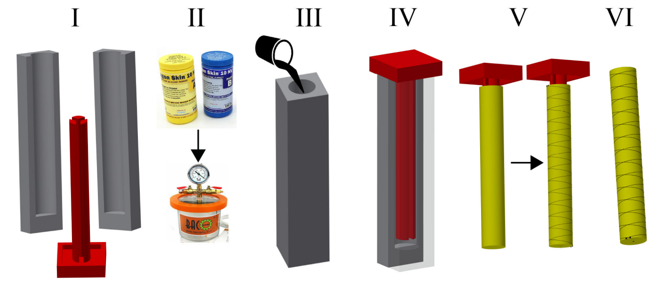

Fig. 9. Fabrication of fiber-reinforced soft actuators: (I) design and 3D print molds, (II) mix and degass silicone rubber (DragonSkin10), (III) clamp molds and pour rubber, (IV) insert inner mold, (V) remove outer molds, add fiber wrapping, and (VI) remove soft actuator and cap top end.

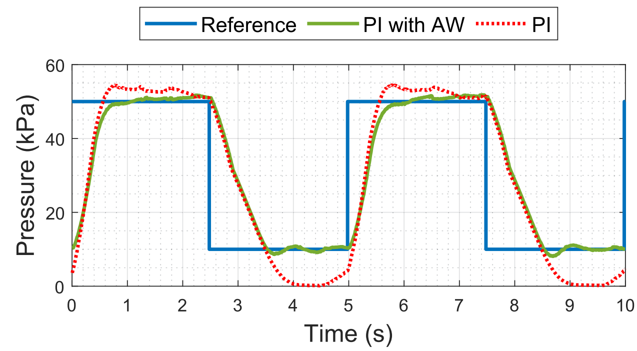

(a) Cownose ray-inspired actuator, $K_p = 0.02$ and $K_i = 0.33$.

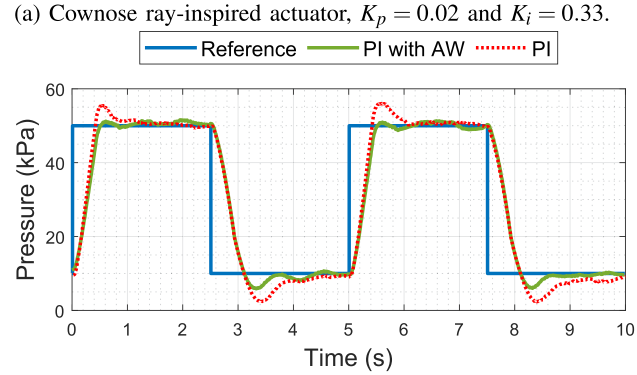

(b) Slow PneuNet actuator, $K_p = 0.02$ and $K_i = 1.11$.

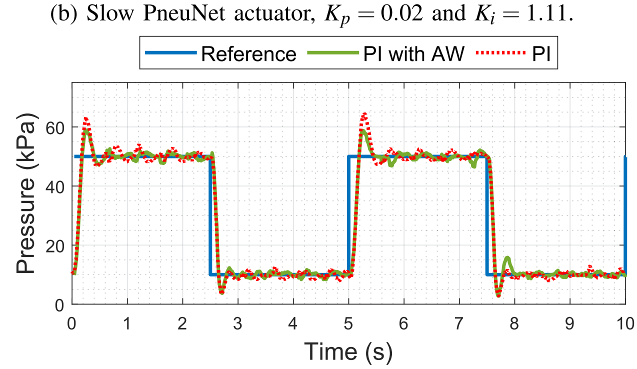

(c) Fiber-reinforced actuator, $K_p = 0.005$ and $K_i = 0.42$.

Fig. 10. Comparison between PI controllers and PI controllers with anti-windup (AW) for a range of soft pneumatic actuators.

(Fig. 8) using myRIO and LabVIEW, and compared to simulation results. The LabVIEW subroutines are available at [33] for both 3/2 and 2/2 valve systems.

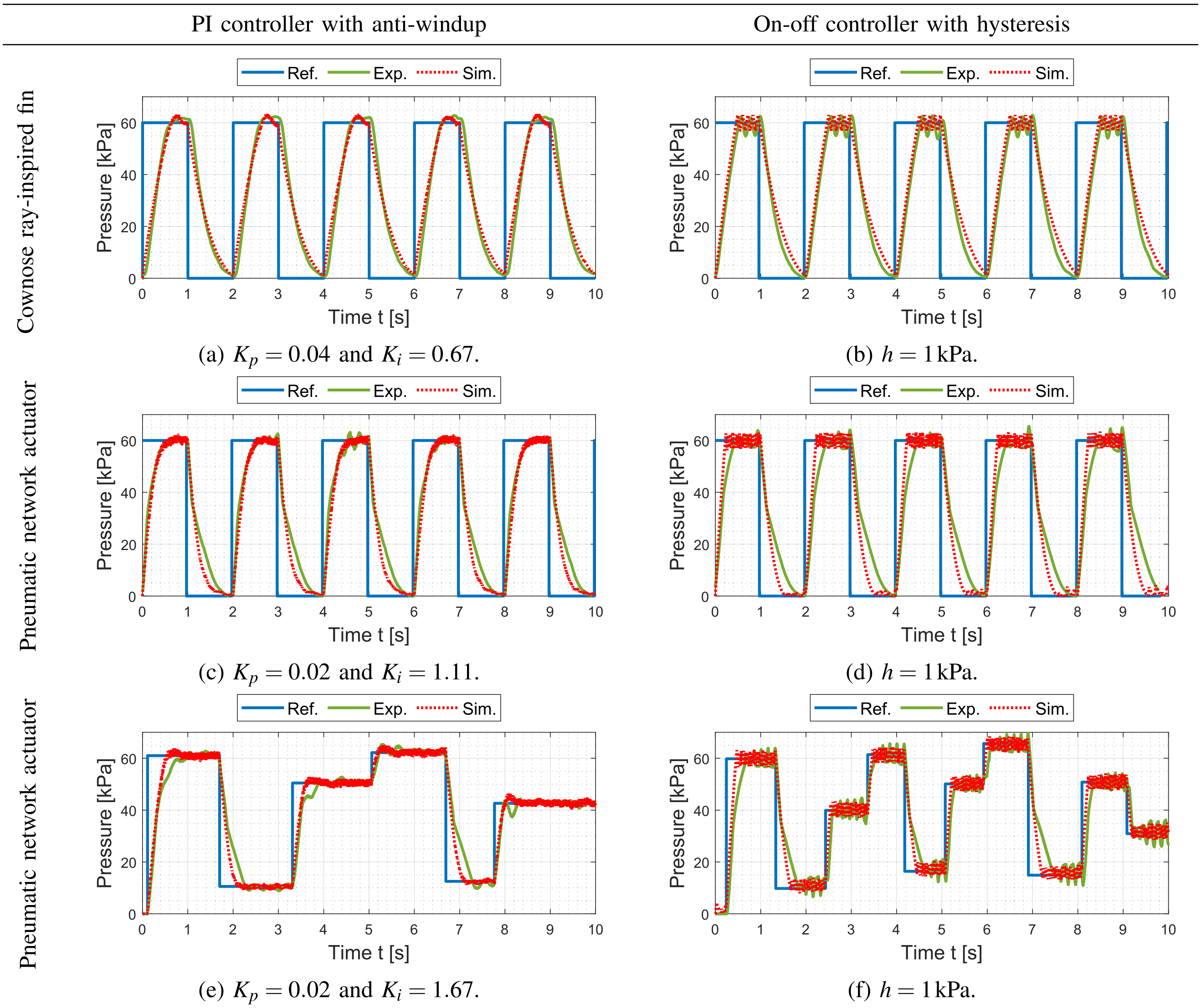

(a) $K_p = 0.04$ and $K_i = 0.67$. (b) $h = 1\,\text{kPa}$.

(c) $K_p = 0.02$ and $K_i = 1.11$. (d) $h = 1\,\text{kPa}$.

(e) $K_p = 0.02$ and $K_i = 1.67$. (f) $h = 1\,\text{kPa}$.

Fig. 11. Comparison between PI controller with anti-windup and on-off controller with hysteresis for pressure tracking. Experimental and simulation results are shown in green and red, respectively. The rise time of 0.5 s designed for the cownose ray-inspired fin is observed in (a) and (b). Additional results are presented for the slow PneuNet in (c)-(f), which shows rise time below 0.5 s due to the lower volume.

A. Fabrication of Soft Pneumatic Actuators

The fabrication process for the omnidirectional actuator is described in Fig. 9 [25]. Molds are designed in Autodesk Inventor and printed using an Original Prusa i3 MK3S (Prusa Research). For the PneuNet actuators, the mixture is poured into the bottom mold after step II and the top mold is inserted. Then, the soft actuator is removed from the molds and a strain limiting layer of fabric is added.

B. Parameter Selection: Application Example

Step 1: $P_A = 60\,\text{kPa}$ (161.325 kPa absolute), $V_A = 60\,\text{mL}$, $T_{rise} = 0.5\,\text{s}$ and $N = 30$ cycles/min.

Step 2: $V_R = 1\,\text{L}$ and $P_R = 100\,\text{kPa}$.

Step 3: $\bar{C} = 0.55$ (red marker in Fig. 5) $\rightarrow C \geq 0.033\,\text{L/(s} \cdot \text{bar)}$.

Step 4: 3/2 valve. From the range of commercial valves, V114 (SMC) is selected with $C = 0.037\text{L/(s} \cdot \text{bar)}$ and $b = 0.11$.

Step 5: From (9) and Fig. 7 (red marker), $Q_{Pump}(P_R) \geq 0.6 + 1.4 = 2\,\text{LPM} \rightarrow$ KYK50BPM or BTX Connect.

The setup investigated here employs the diaphragm pump KYK50BPM, two pressure sensors (SEN0257, DFRobot) and tubing between each of these elements. The PWM output for the motor is connected to a motor driver (VNH5019A) and the PWM outputs for the valves are each connected to a BJT transistor (TIP31 A) through a 330 Ω resistor. A flyback diode (1n5817) is added to dissipate voltage spikes during transistor switching.

C. PI Controller With Anti-Windup

The effect of anti-windup in the PI controllers for the soft pneumatic actuators is presented in Fig. 10. The inclusion of anti-windup has a more significant impact for actuators with larger volumes. For the ray-inspired actuator, the response is slow to recover after a step change due to actuator saturation and integrator windup. However, this is significantly improved

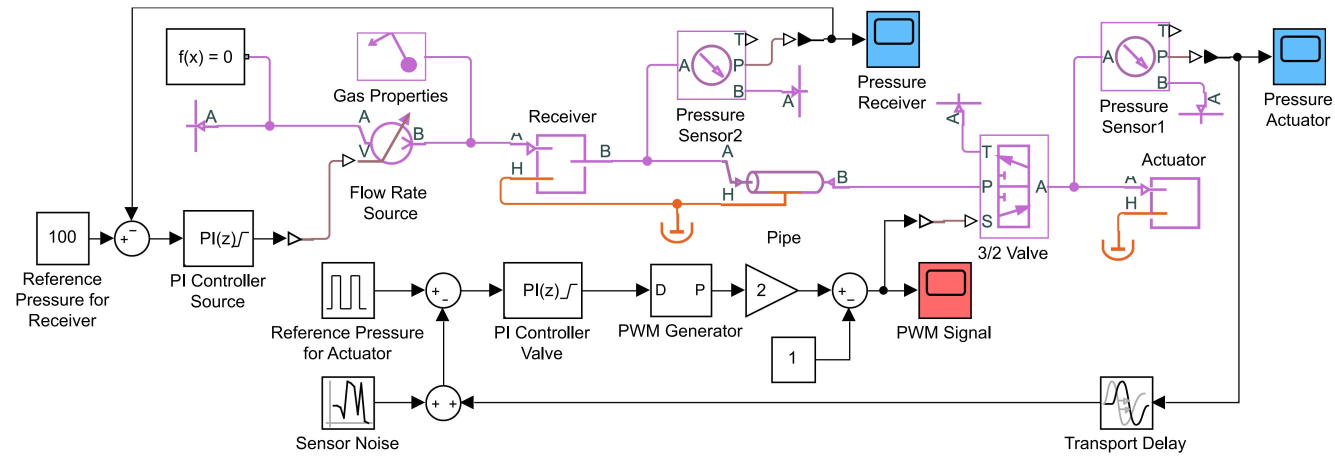

Fig. 12. Model of pneumatic control system in Simulink. The diaphragm pump is modeled as a volumetric flow rate source, the pneumatic line as a pipe, and the air receiver and actuator as constant volume chambers. Pressure sensors are added to the actuator and receiver. Transport delay and random sensor noise are added to the pressure measurements.

when conditional integration is added, which results in lower overshoot and settling time.

D. Comparison of Experimentally-Tuned Controllers

The performance of experimentally-tuned PI controllers with anti-windup and on-off controllers with hysteresis is evaluated for square waves in Figs. 11(a)–(d), which demonstrates the maximum rise time of 0.5 s. These control strategies do not require a periodic signal and can easily account for unstructured reference signals, as shown in Figs. 11(e)–(f). The results demonstrate the ability of both controllers to track dynamic pressure set-points and the versatility of the control approaches. Fluctuations in the pressure response are expected with on-off valves due to oscillations in the internal pressure measurement and finite switching frequency. These oscillations are more significant for actuators with lower volume, as shown in Fig. 10(c).

In comparison to the PI controller, the on-off controller has minimum rise time, however it shows excessive oscillation around the set-point as the pressure oscillates within the hysteresis band. Increasing the hysteresis band degrades the tracking error but advantageously reduces the number of switching events. In many applications, a lower number of switching events and longer valve lifetime may be preferable over minimum tracking error.

Simulations and experimental results show that the PI controller provides smaller tracking error. The on-off controller has a faster rise time but larger pressure oscillation and larger constant tracking error. The requirement for an anti-windup strategy in the PI controller was observed in both simulations and experimental results. The use of conditional integration was observed to reduce overshoot and settling time for the class of systems under consideration, which allows for tracking of rapidly changing references.

Finally, the small discrepancies between simulation and experimental results are a result of the compliance of the soft actuators, which is not taken into account due to the constant volume assumption in the simulations.

VI. Conclusion

This article proposes a systematic approach for selecting pneumatic components to achieve desired closed-loop pressure responses of soft actuators. The results show that by properly sizing the components, appropriate parameter values can be selected to satisfy requirements on the performance of soft actuators and simplify control effort. For the pneumatic systems under consideration, the simulations identify two main physical limitations. First, the sonic conductance of the valve needs to be sufficiently large. Second, the receiver pressure needs to be sufficiently above the range of required actuator pressures. A high pressure difference between the receiver and actuator is observed to reduce the rise time but increase the overshoot and settling time.

Appendix
Simscape Fluids

The pneumatic components are shown in magenta and include the flow rate source, receiver, pipe, 3/2 solenoid valve and the soft actuator. The actuator is modeled as a constant volume chamber. PI controllers are included for pressure regulation at the receiver and actuator. For the on-off controller with hysteresis, the PI block and PWM generator are replaced with a relay. For the dual 2/2 valve system, two relays or PI controllers with complementary PWM waves can be employed. The effects of processing time, discretization delay and measurement delay are incorporated by the transport delay block.

References

[1] D. Trivedi, C. Rahn, W. Kier, and I. Walker, “Soft robotics: Biological inspiration, state of the art, and future research,” *Appl. Bionics Biomech.*, vol. 5, no. 3, pp. 99–117, 2008.

[2] C. Majidi, “Soft-matter engineering for soft robotics,” *Adv. Mater. Technol.*, vol. 4, no. 2, 2019, Art. no. 1800477.

[3] B. Gorissen, D. Reynaerts, S. Konishi, K. Yoshida, J.-W. Kim, and M. De Volder, “Elastic inflatable actuators for soft robotic applications,” *Adv. Mater.*, vol. 29, no. 43, 2017, Art. no. 1604977.

[4] P. Polygerinos *et al.*, "Soft robotics: Review of fluid-driven intrinsically soft devices; manufacturing, sensing, control, and applications in human-robot interaction," *Adv. Eng. Mater.*, vol. 19, no. 12, 2017, Art. no. 1700016.

[5] M. S. Xavier, A. J. Fleming, and Y. K. Yong, "Finite element modeling of soft fluidic actuators: Overview and recent developments," *Adv. Intell. Syst.*, vol. 3, no. 2, 2020, Art. no. 2000187.

[6] C. Tawk and G. Alici, "Finite element modeling in the design process of 3 d printed pneumatic soft actuators and sensors," *Robotics*, vol. 9, no. 3, p. 52, 2020.

[7] E. H. Skorina, M. Luo, S. Ozel, F. Chen, W. Tao, and C. D. Onal, "Feedforward augmented sliding mode motion control of antagonistic soft pneumatic actuators," in *Proc. IEEE Int. Conf. Robot. Automat.*, 2015, pp. 2544–2549.

[8] C. Chen, W. Tang, Y. Hu, Y. Lin, and J. Zou, "Fiber-reinforced soft bending actuator control utilizing on/off valves," *IEEE Robot. Autom. Lett.*, vol. 5, no. 4, pp. 6732–6739, Oct. 2020.

[9] S. Joshi and J. Paik, "Pneumatic supply system parameter optimization for soft actuators," *Soft Robot.*, vol. 8, no. 2, pp. 152–163, 2020.

[10] M. S. Xavier, A. J. Fleming, and Y. K. Yong, "Modelling and simulation of pneumatic sources for soft robotic applications," in *Proc. IEEE/ASME Int. Conf. Adv. Intell. Mechatronics*, pp. 916–921, 2020.

[11] E. H. Skorina, M. Luo, W. Tao, F. Chen, J. Fu, and C. D. Onal, "Adapting to flexibility: Model reference adaptive control of soft bending actuators," *IEEE Robot. Autom. Lett.*, vol. 2, no. 2, pp. 964–970, Apr. 2017.

[12] T. George Thuruthel, Y. Ansari, E. Falotico, and C. Laschi, "Control strategies for soft robotic manipulators: A survey," *Soft Robot.*, vol. 5, no. 2, pp. 149–163, 2018.

[13] M. Wehner *et al.*, "Pneumatic energy sources for autonomous and wearable soft robotics," *Soft Robot.*, vol. 1, no. 4, pp. 263–274, 2014.

[14] J. W. Booth, J. C. Case, E. L. White, D. S. Shah, and R. Kramer-Bottiglio, "An addressable pneumatic regulator for distributed control of soft robots," in *Proc. IEEE Int. Conf. Soft Robot.*, 2018, pp. 25–30.

[15] T. Wang, Y. Zhang, Z. Chen, and S. Zhu, "Parameter identification and model-based nonlinear robust control of fluidic soft bending actuators," *IEEE/ASME Trans. Mechatron.*, vol. 24, no. 3, pp. 1346–1355, Jun. 2019.

[16] C. Onal and D. Rus, "Autonomous undulatory serpentine locomotion utilizing body dynamics of a fluidic soft robot," *Bioinspir. Biomim.*, vol. 8, no. 2, 2013, Art. no. 026003.

[17] A. A. Calderón, J. C. Ugalde, J. C. Zagal, and N. O.Pérez-arancibia, "Design, fabrication and control of a multi-material-multi-actuator soft robot inspired by burrowing worms," in *Proc. IEEE Int. Conf. Rob. Biomimetics*, 2016, pp. 31–38.

[18] A. D. Marchese, C. D. Onal, and D. Rus, "Autonomous soft robotic fish capable of escape maneuvers using fluidic elastomer actuators," *Soft Robot.*, vol. 1, no. 1, pp. 75–87, 2014.

[19] K. Suzumori, S. Endo, T. Kanda, N. Kato, and H. Suzuki, "A bending pneumatic rubber actuator realizing soft-bodied manta swimming robot," in *Proc. IEEE Int. Conf. Robot. Automat.*, 2007, pp. 4975–4980.

[20] S. Ibrahim, J. C. Krause, and A. Raatz, "Linear and nonlinear low level control of a soft pneumatic actuator," in *Proc. IEEE Int. Conf. Soft Robot.*, 2019, pp. 434–440.

[21] M. Memarian, R. Gorbet, and D. Kulić, "Control of soft pneumatic finger-like actuators for affective motion generation," in *Proc. IEEE/RSJ IEEE Int. Conf. Intell. Robots Syst.*, 2015, pp. 1691–1697.

[22] D. Drotman, M. Ishida, S. Jadhav, and M. Tolley, "Application-driven design of soft, 3-d printed, pneumatic actuators with bellows," *IEEE/ASME Trans. Mechatron.*, vol. 24, no. 1, pp. 78–87, Feb. 2019.

[23] A. H. Khan and S. Li, "Sliding mode control with pid sliding surface for active vibration damping of pneumatically actuated soft robots," *IEEE Access*, vol. 8, pp. 88793–88800, 2020.

[24] A. H. Khan, Z. Shao, S. Li, Q. Wang, and N. Guan, "Which is the best pid variant for pneumatic soft robots? an experimental study," *IEEE/CAA J Automatica Sinica*, vol. 7, no. 2, pp. 451–460, Mar. 2020.

[25] M. S. Xavier, A. J. Fleming, and Y. K. Yong, "Image-guided locomotion of a pneumatic-driven peristaltic soft robot," in *Proc. IEEE Int. Conf. Rob. Biomimetics*, 2019, pp. 2269–2274.

[26] M. Luo *et al.*, "Toward modular soft robotics: Proprioceptive curvature sensing and sliding-mode control of soft bidirectional bending modules," *Soft Robot.*, vol. 4, no. 2, pp. 117–125, 2017.

[27] G. C. Goodwin *et al.*, *Control System Design*. Englewood Cliffs, NJ, USA: Prentice Hall, 2001, vol. 240.

[28] K. J. Åström and T. Hägglund, *Advanced PID Control*. Research Triangle Park, NC, USA: ISA, 2006.

[29] J. T, *Pneumatics: Concepts, Design and Applications*. Hyderabad, India: Universities Press, 2015.

[30] P. Beater, *Pneumatic Drives*. Berlin, Germany: Springer, 2007.

[31] D. S. Naidu, *Optimal Control Systems*. Boca Raton, FL, USA: CRC press, 2018.

[32] J. Watton, *Fluid Power Systems: Modeling, Simulation, Analog and Microcomputer Control*. Englewood Cliffs, NJ, USA: Prentice-Hall, Inc., 1989.

[33] T. Young, M. Xavier, A. Fleming, and Y. Yong, "A Control and Drive System for Pneumatic Soft Robots: Pneusord," 2020. [Online]. Available: https://github.com/PrecisionMechatronicsLab/PneuSoRD